

Parametric roll of container ships in head waves

Hisham Moideen, Jeffrey M. Falzarano and S.Abhilash Sharma*

Department of Ocean Engineering, Texas A&M University, College Station, Texas, USA, 77843

(Received June 7, 2012, Revised October 30, 2012, Accepted November 1, 2012)

Abstract. Analysis of ship parametric roll has generally been restricted to simple analytical models and sophisticated time domain simulations. Simple analytical models do not capture all the critical dynamics while time-domain simulations are often time consuming to implement. The model presented in this paper captures the essential dynamics of the system without over simplification. This work incorporates various important aspects of the system and assesses the significance of including or ignoring these aspects. Special consideration is given to the fact that a hull form asymmetric about the design waterline would not lead to a perfectly harmonic variation in metacentric height. Many of the previous works on parametric roll make the assumption of linearized and harmonic behaviour of the time-varying restoring arm or metacentric height. This assumption enables modelling the roll motion as a Mathieu equation. This paper provides a critical assessment of this assumption and suggests modelling the roll motion as a Hills equation. Also the effects of non-linear damping are included to evaluate its effect on the bounded parametric roll amplitude in a simplified manner.

Keywords: parametric roll; container ships; head seas rolling; regular waves

1. Introduction

It is well known that most hull forms especially container ships, Ro-Ro ships and fishing trawlers prone to parametric roll instability are asymmetric about their design water lines. Hence the variation in the metacentric height will be asymmetric as well. This asymmetry invalidates the harmonic approximation. Studies by other researchers (Shin *et al.* 2004, Spyrou 2000) have shown that the harmonic assumption is very crude.

Many of the past research on ship parametric roll have been to predict the occurrence of parametric roll. Fewer analytical methods have been developed to predict the resulting roll amplitude. Some studies were done by (Bulian 2006). In his study a harmonic form was assumed for the response with a slowly varying amplitude and phase. However this required a complicated calculation and statistical linearization. Due to the large amplitude of motion resulting from the parametric instability the effects of non-linear damping also become important. Non-linear damping controls the bounded roll motion amplitude. So far there have been very few attempts to incorporate the effects of non-linear damping into analytical model to predict roll motion amplitude. Many researchers have attempted to evaluate the effects of non-linear damping using time simulations which is very time consuming and does not help in understanding the behaviour of the non-linearity throughout the entire domain.

*Corresponding author, Dr., E-mail: s.abhilash89@gmail.com

Ships typically have varying forward speeds and hence varying encounter or exciting frequency. This property of ships makes them susceptible to both sub and super harmonic parametric resonance and possible instability as compared to offshore structures. Perturbation methods and harmonic assumption greatly affect the domain under which boundaries between the stable and unstable regions are valid. Extending the model to higher harmonics will enable accurate prediction over the entire range of operation. Such simple yet more accurate models can be used as benchmarks to predict parametric instability as well as bounded roll motion amplitude which in-turn can be utilized in the preliminary design stage so as to avoid hull forms prone to parametric rolling.

1.1 Background

Of all the motions, of ship the roll motion is perhaps the most studied because of the issue of stability and also of the disastrous consequences of failure. Large amplitude ship rolling motions can lead to progressive flooding and may eventually lead to the capsizing or foundering of a ship. The issue of stability arises due to the fact that the damping in the roll mode is generally very small which leads to large roll amplitudes and there is a strong softening spring effect on the stiffness which causes a decrease in stiffness at large roll amplitudes. These two effects in tandem pose a serious threat to the stability of the ship. As the radiation damping is usually very small, the ships are outfitted with appendages like bilge keels to provide a non linear viscous damping to limit the roll motion. Hence many studies have been carried out to predict ship roll motion in regular seas.

The beam sea condition is believed to produce maximum rolling and hence has been extensively analyzed, for e.g., (Nayfeh 1986). Falzarano (1990) analyzed the complicated dynamics involved in roll motion leading to capsize using the Melnikov method. The beam seas rolling can be controlled with additional dampening such as that provided by bilge keels, roll tanks, stabilizing fins, etc. Further innovative techniques of utilizing numerical continuation methods and Poincaré Mapping were applied to ship rolling motion by Falzarano *et al.* (1995).

Apart from the beam sea capsizing condition, capsizing in the astern or following seas has also been analyzed (Hamamoto *et al.* 1996, Paulling 1961, Umeda *et al.* 1995). Also recently head seas conditions are being analyzed especially for container ships and ro-ro vessels (Neves and Rodriguez 2006). In the cases of head seas and following seas, there is no direct excitation of the roll motion. Yet there have been reports where it was reported that the head seas caused a large excitation (France *et al.* 2003). This form of excitation where there is no direct excitation but the motion is excited by a change in a parameter of the system (in this case the roll stiffness or GM variation in waves) is called parametric excitation. Parametric rolling is a form of parametric vibration due to time varying stiffness. Studies have shown that for some ships this phenomenon can lead to larger amplitude rolling motion in comparison to the beam seas condition. The change in the underwater hull form and hence the variation of the righting lever in waves leads to a time varying stiffness. If the variation in stiffness is large enough, it can result in large amplitude motion and eventual capsizing. Numerical modelling of parametric rolling of ships in regular waves has been studied widely by Bulian *et al.* (2004), Munif and Umeda (2006), Umeda *et al.* (2004).

The Mathieu instability criterion is the most common method used to determine the onset of parametric roll. Most of the studies have been done with stability charts that do not indicate the

effects of damping. Damping dramatically affects the boundaries between the stable and unstable region. Among container ships the post-Panamax container ship (C11 class) is the most studied vessel as a result of the cargo damage it suffered in 1998 (France *et al.* 2003). Spyrou *et al.* (2008) also studied the prediction possibility of the parametric rolling for the post Panamax container ships.

This current paper reviews the methods commonly used to study parametric roll. One of the most common methods is to use the simple Ince-Strutt stability diagram for Mathieu's equation in predicting the onset of parametric roll. A major drawback of that method is that the Ince-Strutt diagram for Mathieu's equation is generic and does not depend on the ship characteristics. A stability chart which depends on the ship parameters would be an accurate approach.

Since parametric excitation can lead to large amplitude roll motion, the effects of non-linear damping cannot be neglected. Nonlinear roll damping may lead to bounded motion. Hence incorporating the effects of non-linear damping into stability charts would give a more realistic prospect of predicting roll behaviour. Hence without getting into complicated analysis, we can analyze the occurrence of parametric roll and also predict the roll motion amplitude using these charts at an early design stage.

2. Equations of motion

A general equation of motion representing all the six degrees of freedom (surge, sway, heave, roll, pitch and yaw) of any ship is given by Eq. (1).

$$[M]\{\ddot{\xi}\} = \{F\} \quad (1)$$

$[M]$ represents the mass matrix and is in general full matrix coupling all the degrees of freedom. $\{\xi\}$ is a 6×1 vector representing the generalized coordinate vector with each element of the vector representing the motion in one degree of freedom. $\{F\}$ is also a 6×1 vector representing the external forces and moments acting on the ship in each of the degrees of freedom. The force vector is composed of diffraction forces, radiation forces, viscous forces and restoring forces as shown in Eq. (2).

$$[M]\{\ddot{\xi}\} = \{F_{Diff}\} + \{F_{Rad}\} + \{F_{Visc}\} + \{F_{Res}\} \quad (2)$$

The radiation, viscous and restoring forces can be expressed in terms of the ship motions and are usually transferred to the left hand side of the equation resulting in Eq. (3).

$$[M+A]\{\ddot{\xi}\} + [B]\{\dot{\xi}\} + [C(\{\xi\},t)] = \{F_{Diff}\} \quad (3)$$

$[A]$ and $[B]$ represent the added mass and damping matrices and $[C]$ represents the stiffness matrix which in the most general case is dependent of the position and time.

In this paper our focus is primarily on the roll motion. As observed from above, roll ($\{\xi_4\}$) equation of motion is coupled with all of the other motions through inertial terms (including added mass and coordinate coupling terms) and radiation damping terms.

For simplification of analysis a set of assumptions are made to decouple the roll equation of

motion from the other degrees of freedom. Firstly, from the linear hydrostatics it can be observed that there is no restoring force in the surge, sway and yaw directions (horizontal plane motions) and hence these motions do not have any stiffness coupling (coupling in $[C]$ matrix) with roll, pitch and heave (vertical plane motions). As the waves are assumed to be incident head on, there is no direct excitation in roll, sway and yaw motions. Thus the responses in sway and yaw are assumed to be significantly small so that roll motion can be considered to be completely decoupled from horizontal plane motions.

Due to the symmetry of the ship about the center line and by choosing an appropriate body fixed coordinate system, the stiffness and inertial coupling between roll and heave motion can be eliminated. This choice of coordinate system would also reduce the inertial coupling between roll and pitch. Thus in lieu of examining the effects of parametric roll the effects of the coupling terms in added mass and damping are insignificant and hence neglected. Thus, under the above made assumptions, the roll equation of motion is completely decoupled and can be expressed as Eq. where damping has been linearized and only the linear hydrostatic stiffness is retained.

$$(I + A(\omega))\ddot{\phi} + (B(\omega))\dot{\phi} + C(t, \phi) = 0 \quad (4)$$

where

ϕ denotes the roll angle,

I and A represent the roll moment of inertia and added moment of inertia

B represents the damping

$C(t, \phi)$ represents the roll restoring stiffness

ω is the forcing frequency

The stiffness in the Eq. is retained as a function of time because as a wave passes through, the underwater hull form changes and thus leads to a change in roll stiffness c with time. Linearized stiffness (i.e., the GM) can further be expressed as in Eq. (5)

$$C(t, \phi) = \Delta g GZ(t, \phi) \quad (5)$$

where $GZ(t, \phi)$ is the time varying roll restoring arm. The righting arm is generally approximated as an odd polynomial function (due to the symmetry of the ship about the centreline) of the roll angle as in Eq. (6). In this paper, for a simplified analysis only the first order restoring arm (GM) shall be considered which is assumed to be composed of still water $GM(GM_0)$ and a time varying part ($\delta GM(t)$) (Eqs. (7) and (8)). Thus the equation of motion is now given by Eq. (9).

$$GZ(t, \phi) = C_1(t)\phi + C_3(t)\phi^3 + C_5(t)\phi^5 + \dots \quad (6)$$

$$\begin{aligned} GZ(t, \phi) &= C_1(t)\phi \\ &= GZ(t, 0) + \frac{\partial GZ}{\partial \phi}(t)\phi + O(\phi^2) \end{aligned} \quad (7)$$

$$= GZ(t)\phi$$

$$GM(t)\phi = (GM_0 + \delta GM(t))\phi \quad (8)$$

$$(I + A(\omega))\ddot{\phi} + (B(\omega))\dot{\phi} + \Delta g(GM_0 + \delta GM(t))\phi = 0 \tag{9}$$

If $\delta GM(t) = \delta GM \cos(\omega t)$ then using the following transformation (Eqs. (10) and (11)) Eq. (9) is transformed into a non-dimensional form - Eq. (12).

$$\tau = \omega t, \omega_D = \sqrt{\frac{g\Delta GM_0}{(I + A(\omega))}}, (\cdot)' = \frac{d}{d\tau} \tag{10}$$

$$\alpha = \left(\frac{\omega_D}{\omega}\right)^2, \gamma = \frac{\delta GM}{GM_0}\alpha, \mu = \frac{B(\omega)}{(I + A(\omega))\omega} \tag{11}$$

$$\frac{d^2\phi}{d\tau^2} + \mu\frac{d\phi}{d\tau} + (\alpha + \gamma\cos(\tau))\phi = 0 \tag{12}$$

Eq. (12) represents a typical damped Mathieu type equation. The stability zones of the above equation are given by the Mathieu Stability Chart or the Ince-Strutt diagram which helps determine the occurrence of parametric vibration. A typical Mathieu Stability Chart for the damped ($\mu > 0$) is shown in Fig. 1. The shaded regions denote the unstable region where the system would be unstable and the vibration amplitude would progressively increase with time. The procedure to develop the Mathieu Stability Chart is described in detail in (Moideen 2011, Moideen 2012) and is also presented in Appendix A of this paper.

The Mathieu Stability Chart plots the stable and unstable zones in the α - γ plane, where α is measure of the still water GM tuning (GM_0) while γ is a measure of the variation of GM in waves (δGM). It is evident from Fig. 1 that larger the values of γ (larger variation of GM in waves) it is more probable that the ship falls in one of the unstable zones and undergoes parametric excitation. In terms of energy one can imagine damping tending to drain the energy from the excitation until the threshold energy is reached to instigate parametric vibration. Hence one method of avoiding parametric roll in ships would be to increase the damping.

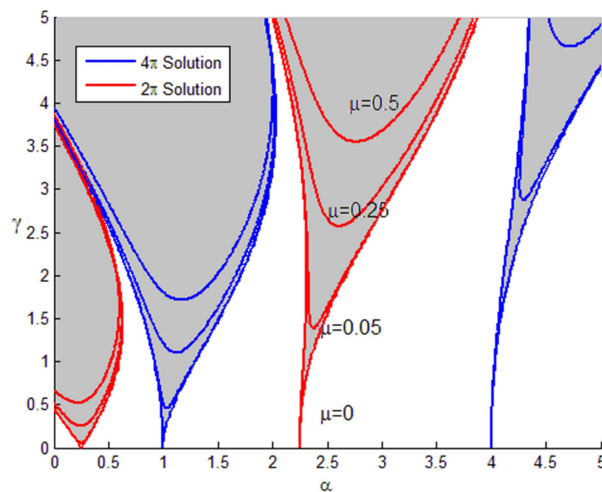


Fig. 1 Ince-strutt diagram or mathieu stability chart

The advantage of the above chart is that it can be used to study the parametric instability of any dynamical system whose equation of motion can be modelled as a Mathieu equation. This is so because the charts are not affected by the parameters of the system under study. Depending on where the ordered pair falls in the chart, it becomes trivial to predict the occurrence of parametric instability.

However, if the stiffness variation is not single frequency harmonic and sinusoidal the system cannot be represented by a Mathieu equation. In such a case we can always represent the time varying coefficient (stiffness for ships) as a Fourier expansion. The resulting equation is called Hill's Equation. Since the formulation of the Hill's equation depends on ship parameters, these charts give a better prediction model. More information on dependence of the Hill's coefficients on the hull properties is given in (Moideen 2012)

3. The variation of stiffness in waves for container ships

It is evident from the previous discussion that as the variation of GM in waves increases, it is more likely that the vessel would undergo a parametric excitation. Modern container ships often fit the criteria of having a large variation of GM in waves. These ships have a fine underwater hull form with a flare forward and a broad flat transom stern. Thus, when the wave crest is amidships, the waterplane width in the forward and aft reduces considerably, while it remains constant amidships. On the contrary, when the wave trough is at amidships, the immersion of the forward flare and transom stern cause the waterplane area to increase. Thus the initial stability (GM) with wave crest amidships is much lower than with wave trough amidships leading to the large variation of GM in waves.

For the purpose of generating the stability charts, a slightly modified post panamax C11 hull form, which has been known to exhibit parametric rolling (France *et al.* 2003), has been chosen. The stern of the hull has been modified to have a fuller form, and this model is named Pram aft body (Moideen 2012). The main particulars of the vessel are listed in Table 1.

The fine underwater form, flare forward and broad flat transom of the modified C11 can be seen in Figs. 2 and 3. The significant change in underwater hull form is evident in Fig. 4.

In order to estimate the GM variation in regular waves, the roll restoring curve (GZ) for 10 different wave-crest positions along the ship are calculated. Standard hydrostatic software is used to obtain the GM for the different wave crest positions. Calculations are done for zero forward speed and free trim condition (hydrostatic balance). The details of the regular wave used for calculation are given below,

$$\text{Wavelength } \lambda = L_{pp} = 262 \text{ m}$$

$$\text{Wave Number } k = \frac{2\pi}{\lambda} = 0.024 \text{ m}^{-1}$$

For deep water, the wave frequency is given by

$$\omega^2 = gk \quad (13)$$

$$\omega = \sqrt{gk} = \sqrt{9.81 * 0.024} = 0.485 \text{ rad/s} \quad (14)$$

Table 1. Main particulars of C11 hull form (pram aft body)

| Particulars | Details |
|------------------------------------|----------|
| L_{p-p} (m) | 262.00 |
| B (m) | 40.00 |
| D (m) | 24.45 |
| Mean Draft (m) | 11.50 |
| Displacement (tones) | 69128.00 |
| KG (m) | 18.37 |
| GMt (m) | 1.96 |
| Natural Roll Period, $T\Phi$ (sec) | 25.14 |

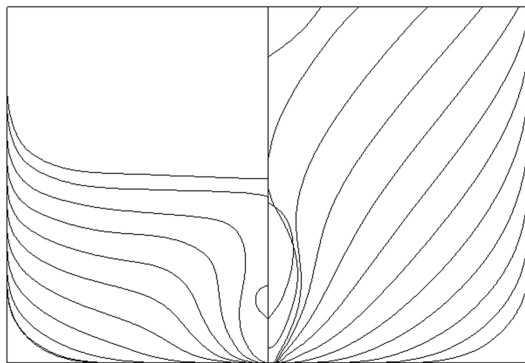


Fig. 2 Body plan of modified C11 hull form (not to scale)

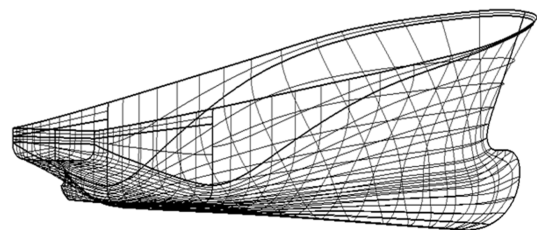


Fig. 3 Wire mesh model of modified C11 hull

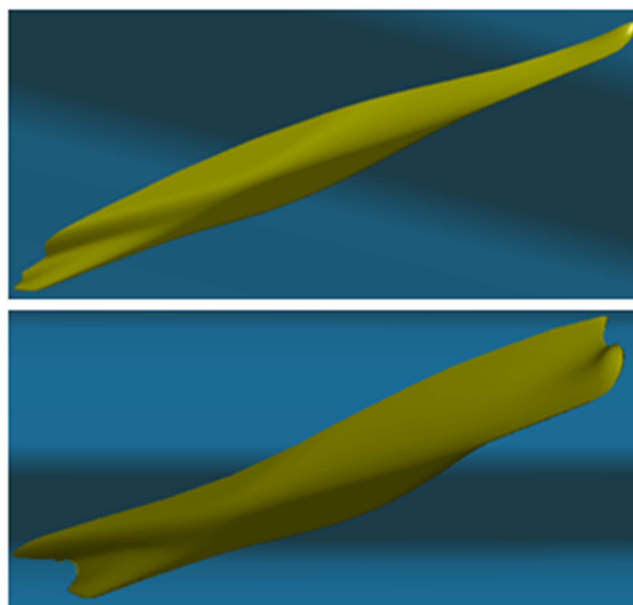


Fig. 4 Change in underwater hull form in waves of modified C11 hull form

The ship’s natural frequency of roll is given by $\omega_n = 0.25 \text{ rads/sec}$. The damping ratio is given by Eq. (15).

$$\xi = \frac{B(\omega_n)}{(I+A(\omega_n))} \sim 0.003 \Rightarrow \omega_D = \omega_n \sqrt{1-\xi^2} \sim \omega_n \tag{15}$$

Hence the parameter, $\alpha = \left(\frac{\omega_D}{\omega}\right)^2 \sim \left(\frac{\omega_n}{\omega}\right)^2 = 0.265$

It is evident from Fig. 1 that this value is quite close to the principal parametric resonance zone ($\alpha = 0.25$).

A wave height equal to 1/40 of wavelength is used to estimate GM, $H_w = 6.55 \text{ m}$. The effect of non-linear coupling due to pitch and heave on the hydrostatics of the vessel is neglected. Fig. 5 represents the variation of GM as a function of the position of the wave crest, calculated for the above mentioned wave.

This variation is generally represented with a cosine fit to yield the Mathieu equation. However, as shown in Fig. 6 a cosine fit does not represent the GM variation accurately. (Spyrou

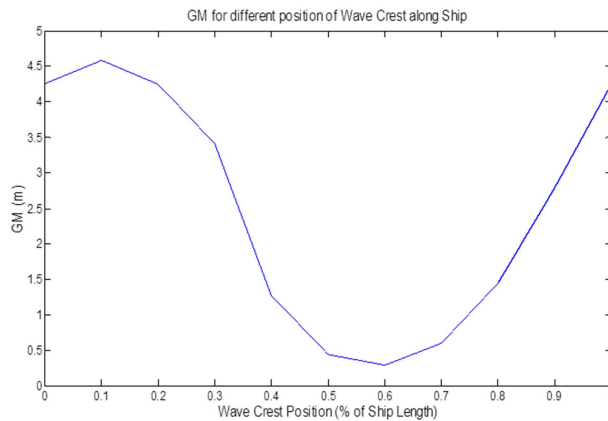


Fig. 5 Variation in GM as the wave crest passes through the hull form

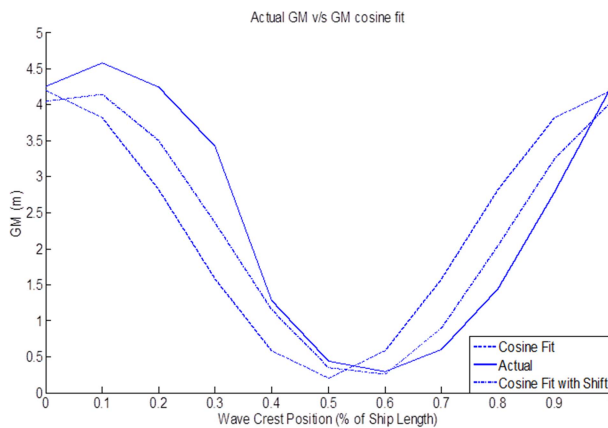


Fig. 6 Comparison of cosine fit of GM with actual GM. (--- Cosine Fit and -.- Cosine Fit with Shift of $\pi/8$)

et al. (2008)[15]) proposed that a case of cosine fit with a phase shift has a better fit (Fig. 6 uses a phase shift of $\pi/8$ for the plot of cosine fit with a phase shift). Even the phase shifted cosine fit does not accurately depict the GM variation.

Thus, there is a need to use a method with which the GM variation may be approximated more accurately. This paper investigates the use of Hill's Equation for this purpose. The Hill's Equation is obtained by representing the time varying GM ($\delta GM(t)$) in Eq. (8) as a Fourier series. Thus if the time varying stiffness is represented as in Eq. (16), then utilizing the transformations in Eqs. (10) and (11), the non-dimensional form of the damped Hill's Equation would be given by Eq. (17).

$$\delta GM(t) = \sum_{n=0}^{\infty} C_n \cos(n\tau) + S_n \sin(n\tau) \quad (16)$$

$$\frac{d^2\phi}{d\tau^2} + \mu \frac{d\phi}{d\tau} + \left(\alpha + \gamma \sum_{n=0}^{\infty} A_n \cos(n\tau) + B_n \sin(n\tau) \right) \phi = 0 \quad (17)$$

Similar to Mathieu Stability Charts, Hill's Stability Charts can also be evaluated. The mathematical procedure to evaluate these charts is similar to the development of the Mathieu Chart and is given in (Moideen 2012) and is also presented in Appendix B of this paper for the sake of completeness.

4. The effects of damping

4.1 Linear damping

For the damped Mathieu's equation, the curves are lifted off from the α -axis due to the presence of damping. This is clearly evident in Fig. 1. It can be seen that though the linear damping in general reduces the region of instability in the α - γ . The stability curves are pushed away from the α axis, increasing the stability region in the α - γ plane. Thus linear damping always helps reduce the unstable region but does not bound the roll motion in the unstable region.

4.2 Non-linear damping

When the system is in an unstable region of the α - γ plane, the parametric excitation causes increased roll amplitudes. The large amplitude rolling is a complicated phenomenon due to the presence of the non-linear damping in the system. The roll amplitude monotonically increases in the presence of linear damping. As the amplitude increases the effects of the non-linear damping also becomes progressively very important. Due to the presence of the non-linear damping the parametric roll amplitude is then restricted to a limit cycle. The non-linear damping force is the only bounding force which limits the roll motion to a limit cycle. Hence it is important to study the effects of non-linear damping in parametric roll.

In general the various components of the roll damping may be classified as shown in Eq. (18) (Chakrabarti 2001)

$$B_{eq} = B_f + B_e + B_W + B_L + B_{BK} \quad (18)$$

Where

- B_{eq} : Equivalent damping
- B_f : Hull skin friction damping
- B_e : Hull eddy shedding damping
- B_W : Free surface radiated wave damping
- B_L : Lift force damping
- B_{BK} : Bilge Keel damping

In general the non-linear damping terms are coupled to each other and hence are difficult to estimate. However empirical formulas have been developed based on numerous experiments (Himeno 1981). The general practice is to assume the damping to be composed of linear, quadratic and cubic components as shown in Eq. (19).

$$B(\dot{\phi}) = B_1 \dot{\phi} + B_2 \dot{\phi} |\dot{\phi}| + B_3 \dot{\phi}^3 \quad (19)$$

In this paper a linear and quadratic damping has been considered while the cubic damping has been neglected. Thus, the damping is given as in Eq. (20).

$$B(\dot{\phi}) = B_1(\dot{\phi}) + B_2 \dot{\phi} |\dot{\phi}| \sim (B_1 + B_{2,eq}) \dot{\phi} \quad (20)$$

For the purpose of analytical solution, the quadratic damping is non-linear and leads to complications. Hence an equivalent linear form is used to develop the analytical models (Eq. (20)). The equivalent form in the non-dimensional form is shown in Eq. (21).

$$\mu = \mu_1 + \mu_2 R_0 \quad (21)$$

where μ is the Non-Dimensional Linearized Damping Coefficient, μ_1 is the Non-Dimensional Linear Damping Coefficient, μ_2 is the Equivalent Linearized Quadratic Damping Coefficient and R_0 is the Roll Amplitude.

It can be seen that the linearized quadratic damping term is also not strictly linear as it is dependent on the Roll Amplitude at the particular instant. Empirical relations for the calculation of linear damping coefficient and the linearized quadratic damping coefficient are shown in Eqs. (22) and (23) respectively. It can be seen that the damping coefficients depend on α . Thus a formulation of the stability charts for constant linear damping as in Fig. 1 would be incorrect.

$$\mu_1 = \frac{\beta_1(\omega)}{(I + A_{44}(\omega))\omega} = \frac{B_1(\omega)}{(I + A_{44}(\omega))(\omega_D)} \sqrt{\alpha} \quad (22)$$

$$\mu_2 = \frac{8}{3\pi} \frac{B_2(\omega)\omega_D}{(I + A_{44}(\omega))\omega} = \frac{8}{3\pi} \frac{B_2(\omega)\sqrt{\alpha}}{(I + A_{44}(\omega))} \quad (23)$$

Thus the complete equation of motion is given by Eq. (24)

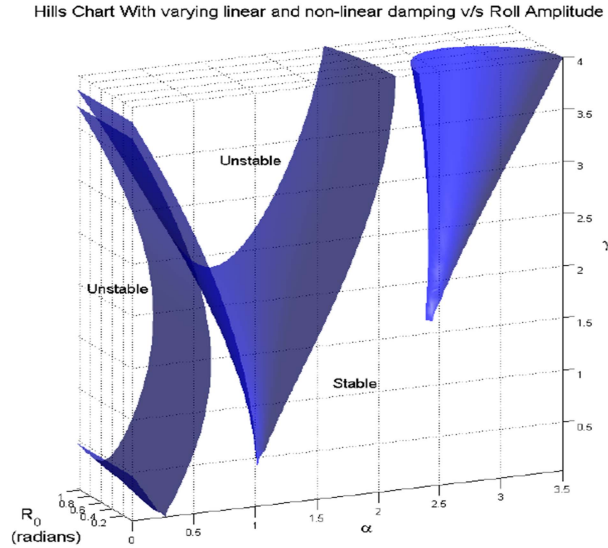


Fig. 7 Hill's stability chart

$$\frac{d^2\phi}{d\tau^2} + (\mu_1 + \mu_2 R_0) \frac{d\phi}{d\tau} + \left(\alpha + \gamma \sum_{n=0}^{\infty} A_n \cos(n\tau) + B_n \sin(n\tau) \right) \phi = 0 \quad (24)$$

As before, Hill's Stability charts can be developed for the above equation for each R_0 . Thus allowing for R_0 to be a parameter in the Hill's Stability Chart leads to a 3-dimensional Stability Chart as shown in Fig. 7.

The advantage of developing such a chart is that once the ship parameter for the particular wave is plotted we can project the point onto the surface and the roll amplitude at which the projection intersects with the surface is the resulting bounded roll motion amplitude due to the parametric excitation with a non-linear damping.

5. The influence of forward speed

Unlike fixed offshore structures, ships move with a forward speed. This brings about a different problem of the instability as the forward speed results in the well-known apparent change in frequency of the waves encountered. Since the parametric roll is a phenomenon dependent primarily on the hull geometry (which causes the large variation of roll restoring stiffness in waves) a perceived change in the incident wave frequency (encounter frequency) would also lead to significant changes to the roll amplitude. It is clear from the previous sections that the parametric excitation is very sensitive to the frequency ratio ($\alpha = \omega_D/\omega^2$). Due to the change in frequency owing to the forward speed, the vessel may experience increase or decrease in the amplitude of parametric roll already present, or even negate the motion depending on the frequency ratio. From a design point it is important to check that the vessel is not in any unstable zone at its operational design speed. Similarly, it is also necessary to observe the effects of changing speed, as changing the heading speed of ship may trigger large parametric rolling.

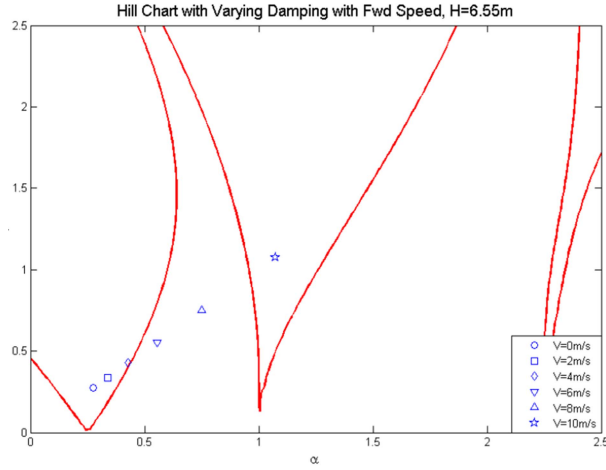


Fig. 8 Effect of forward speed on parametric stability

Considering these consequences, it is necessary to investigate the influence of forward speed on the parametric roll properties of the vessel and to identify the safe speed zones. Also, the studied forward speed influence can be used as a tool for parametric roll stabilization.

The encounter frequency of a vessel moving with forward speed U is given by Eq. (25), where ω , k represent the original frequency and the wave number respectively and β represents the heading angle measured clockwise from the positive x -axis (surge axis).

$$\omega_e = \omega - kU\cos(\beta) \quad (25)$$

Assuming a deep water waves, the encounter frequency can be represented as in Eq. (26). Thus the parametric roll parameter α can be written as in Eq. (27).

$$\omega^2 = gk \Rightarrow \omega_e = \omega - \frac{\omega^2 U}{g} \cos(\beta) \quad (26)$$

$$\alpha = \left(\frac{\omega_D}{\omega_e} \right)^2 = \left(\frac{\omega_D}{\omega - \frac{\omega^2 U}{g} \cos(\beta)} \right)^2 \quad (27)$$

Since the same waves are encountered by the hull as before, the Fourier coefficients of the GM variation will be the same as before. The only change is in the frequency of the GM variation which is equal to the encounter frequency of the waves. Thus the Hill's stability charts are also the same, but the value of α to be checked would change as given above in Eq. (27). The effect of different forward speeds of the vessel is shown in Fig. 8.

According to Faltinsen (1993) the strip theory approximation is valid only up to Froude Number i.e.,

$$F_n = \frac{U}{\sqrt{Lg}} < \approx 0.4. \text{ For the case considered here the Froude number is less than 0.2.}$$

6. Conclusions

The primary reason for fine form container ships and Ro-Ro vessels being prone to large parametric roll is the large variation of the roll stiffness in waves. The analysis carried out in this paper clearly exhibits the usefulness of simple Ince-Strutt diagrams or instability chart in predicting parametric roll of ships. The chart also demonstrates the implicit dependence of the phenomenon of linear and quadratic damping.

The ability of the charts to predict the bounded roll motion amplitude is perhaps a feature so far not discussed. The effects of non-linear damping to limit the motion can be explained using these stability charts. Being able to estimate the bounded roll motion amplitude can be very helpful in the initial design stage to study the implications of parametric roll on the stability of the vessel.

The Hill's equation tends to consider the time varying stiffness more accurately in comparison to the Mathieu and hence the use of a stability diagram for Hill's equations would give a much more precise prediction of the occurrence of parametric roll especially in higher instability zones. The charts can also be used to calculate the critical frequency and the threshold wavelength which would initiate large amplitude rolling motion.

The parametric stability of the vessel for different forward speeds can also be predicted using these improved charts. The charts also enable the study of parametric stabilization. For example by merely increasing or decreasing the speed of the vessel it would be possible to avoid parametric roll or worsen the situation by moving into a more unstable region. These instability charts can act as a guide for crew on-board a ship experiencing large amplitude motion in head/following sea in deciding whether to increase or decrease the vessel speed and to what extent.

Hence apart from serving the purpose of a simple and practical tool for parametric roll study during the initial design stage the Mathieu or Hill stability charts can also be helpful during the operation of the vessel in a seaway.

7. Acknowledgments

The authors would like to thank Dr. Frans van Walree of MARIN for making available to us the hull form description for our analysis.

The work has been funded by Office of Naval Research (ONR) T-Craft tools development program ONR Grant N00014-07-1-1067. Also the authors would like to thank the program manager Ms. Kelly Cooper for her support.

References

- Bulian, G. (2006), *Development of analytical nonlinear models for parametric roll and hydrostatic restoring variations in regular and irregular waves*.
- Bulian, G., Francescutto, A. and Lugni, C. (2004), "On the nonlinear modeling of parametric rolling in regular and irregular waves", *Int. Shipbuild. Prog.*, **51**(2-3), 173-203.
- Chakrabarti, S. (2001), "Empirical calculation of roll damping for ships and barges", *Ocean Eng.*, **28**(7) 915-932.
- Faltinsen, O. (1993), *Sea loads on ships and offshore structures*, Cambridge university press.
- Falzarano, J., Esarza, I. and Tazul mulk, M. (1995), "A combined steady-state and transient approach to study

- large amplitude ship rolling motion and capsizing”, *J. Ship. Res.*, **39**(3), 213-224.
- Falzarano, J. M. (1990), *Predicting complicated dynamics leading to vessel capsizing*, University of Michigan.
- France, W.N., Levadou, M., Treacle, T.W., Paulling, J.R., Michel, R.K. and Moore, C. (2003), “An investigation of head-sea parametric rolling and its influence on container lashing systems”, *Marine Technol.*, **40**(1), 1-19.
- Hamamoto, M., Sera, W., Ito, H., Kan, M., Fujiwara, T., Enomoto, T., Panjaitan, J.P., Takaishi, Y. and Haraguchi, T. (1996), “Model experiments of ship capsize in astern seas second report”, *J. Soc. Naval Architect. Japan*, **179**, 77-87.
- Hayashi, C. (1964), *Nonlinear oscillations in physical systems*, McGraw-Hill New York.
- Himeno, Y. (1981), *Prediction of ship roll damping. a state of the art*, DTIC Document.
- Moideen H. and Falzarano J.M. (2010), “A critical assessment of ship parametric roll analysis”, *Proceedings of the 11th ISSW*, Wageningen, Netherlands, July.
- Moideen, H. (2012), *Prediction of parametric roll of ships in regular and irregular sea*, Text (Thesis), Available: <http://hdl.handle.net/1969.1/ETD-TAMU-2010-12-8692>
- Munif, A. and Umeda, N. (2006), “Numerical prediction on parametric roll resonance for a ship having no significant wave-induced change in hydrostatically-obtained metacentric height”, *Int. Shipbuild. Prog.*, **53**(3), 183-203.
- Nayfeh, A. and Khdeir, A. (1986), “Nonlinear rolling of ships in regular beam seas”, *Int. Shipbuild. Prog.*, **33**(379), 40-49.
- Neves, M.A.S. and Rodríguez, C.A. (2006), “On unstable ship motions resulting from strong non-linear coupling”, *Ocean Eng.*, **33**(14-15), 1853-1883.
- Paulling, J. (1961), “The transverse stability of a ship in a longitudinal seaway”, *J. Ship. Res.*, **4**, 37- 49.
- Shin, Y., Belenky, V.L., Paulling, J.R., Weems, K.M., Lin, W.M., Mctaggart, K., Spyrou, K.J., Treacle, T.W., Levadou, M., Hutchison, B.L., Falzarano, J., Chen, H. and Letizia, L. (2004), “Criteria for parametric roll of large containerships in longitudinal seas. Discussion”, *T. Soc. Naval Architec. Marine Eng.*, **112**, 14-47.
- Spyrou, K. and Thompson, J. (2000), “The nonlinear dynamics of ship motions: a field overview and some recent developments”, *Philos. T. R. Soc. A.*, **358**(1771), 1735-1760.
- Spyrou, K., Tigkas, I., Scanferla, G., Pallikaropoulos, N. and Themelis, N. (2008), “Prediction potential of the parametric rolling behaviour of a post-panamax containership”, *Ocean Eng.*, **35**(11-12), 1235-1244.
- Umeda, N., Takaishi, Y., Matsuda, A., Suzuki, S., Watanabe, K., Hamamoto, M., Chiba, Y., Sera, W. and Spyrou, K. (1995), “Model experiments of ship capsize in astern seas”, *J. Soc. Naval Architec. Japan*, **177**, 207-217.
- Umeda, N., Hashimoto, H., Vassalos, D., Urano, S. and Okou, K. (2004), “Nonlinear dynamics on parametric roll resonance with realistic numerical modelling”, *Int. Shipbuild. Prog.*, **51**(2-3), 205-220.

Appendix A. Mathieu Equation and Stability Charts

Mathieu equation is extensively studied in the field of parametric vibration. There are two primary methods by which the stability charts are generated. The first method is a perturbation technique (Hayashi (1964)). This is an approximation and the validity of these is very limited. The other method is the Hills infinite determinant method which is very accurate in the region they are defined. Also their accuracy can be increased by including more and more terms of the infinite determinant. The standard Mathieu Equation with damping is given by Eq. (A.1).

$$\frac{d^2x}{d\tau^2} + \mu \frac{dx}{d\tau} + (\alpha + \gamma \cos(\tau)) = 0 \quad (\text{A.1})$$

From Floquet theory, the boundaries of the stability and instability are the 2π and 4π periodic solutions. The 2π and 4π periodic solutions of the Mathieu Eq. (A.1) are represented by Eqs. (A.2) and (A.3) respectively.

$$x_{2\pi}(t) = a_0 + \sum_{n=1}^{\infty} (a_n \cos(n\tau) + b_n \sin(n\tau)) \tag{A.2}$$

$$x_{4\pi}(t) = a_0 + \sum_{n=1,3,5\dots}^{\infty} \left(a_n \cos\left(\frac{n\tau}{2}\right) + b_n \sin\left(\frac{n\tau}{2}\right) \right) \tag{A.3}$$

Substituting Eqs. (A.2) and (A.3) into Eq. (A.1) and setting the secular terms to zero yields two matrix equation in the coefficients of the 2π and 4π periodic solutions. These are given in Eqs. (A.4) and (A.5).

$$\begin{bmatrix} \alpha & \frac{\gamma}{2} & 0 & 0 & 0 & \dots & 0 \\ \gamma & \alpha-1 & \mu & \frac{\gamma}{2} & 0 & \dots & 0 \\ 0 & -\mu & \alpha-1 & 0 & \frac{\gamma}{2} & \dots & 0 \\ 0 & \frac{\gamma}{2} & 0 & \alpha-4 & 2\mu & \frac{\gamma}{2} & 0 \\ 0 & 0 & \dots & \dots & \dots & \dots & \dots \end{bmatrix} \begin{bmatrix} \alpha_0 \\ \alpha_1 \\ \alpha_2 \\ b_2 \\ a_3 \\ \dots \end{bmatrix} = 0 \tag{A.4}$$

$$\begin{bmatrix} \alpha - \frac{1}{4} + \frac{\gamma}{2} & \frac{\mu}{2} & \frac{\gamma}{2} & 0 & 0 & \dots & 0 \\ -\frac{\mu}{2} & \alpha - \frac{1}{4} - \frac{\gamma}{2} & \mu & \frac{\gamma}{2} & 0 & \dots & 0 \\ \frac{\gamma}{2} & 0 & \alpha - \frac{9}{4} & \frac{3\mu}{2} & \frac{\gamma}{2} & \dots & 0 \\ 0 & \frac{\gamma}{2} & -\frac{3\mu}{2} & \alpha - \frac{9}{4} & 0 & \frac{\gamma}{2} & 0 \\ 0 & 0 & \dots & \dots & \dots & \dots & \dots \end{bmatrix} \begin{bmatrix} \alpha_0 \\ \alpha_1 \\ \alpha_2 \\ b_2 \\ a_3 \\ \dots \end{bmatrix} = 0 \tag{A.5}$$

Neglecting the trivial case of $a_0 = a_1 = b_1 \dots = 0$, the determinant of the parametric matrix (matrix containing α and γ) should be zero. This gives the relationship between the parameters α and γ . The instability boundaries for various damping ratios are shown in Fig. 1. The shaded region indicates the unstable zone.

Appendix B. hill’s stability charts

The Hill’s equation can be thought of as an extension of the Mathieu equation considering higher order harmonics. The Hill’s equation is given by Eq. (B.1).

$$\frac{d^2 \phi}{d\tau^2} + \mu \frac{d\phi}{d\tau} + \left(\alpha + \gamma \sum_{n=0}^{\infty} A_n \cos(n\tau) + B_n \sin(n\tau) \right) \phi = 0 \tag{B.1}$$

Since the variation in stiffness is periodic we can still apply the Floquet theorem to the Hill’s equation. In order to develop the curves for marginal stability we follow the same procedure as for Mathieu’s equation. Substituting the solution as a Fourier expansion of 2π and 4π periodic terms (Eqs. (A.2) and (A.3)) into Eq. (B.1) and setting the coefficients of secular terms to zero we get the following parametric and coefficient matrix Eqs. (B.2) and (B.3) respectively.

$$\begin{bmatrix} \alpha & \frac{\gamma A_1}{2} & \frac{\gamma B_1}{2} & \frac{\gamma A_2}{2} & \frac{\gamma B_2}{2} & \dots & 0 \\ \gamma A_1 & \alpha - 1 & \mu + \frac{\gamma B_2}{2} & \frac{\gamma(A_3 + A_1)}{2} & \frac{\gamma(B_3 + B_1)}{2} & \dots & 0 \\ \gamma B_1 & \frac{\gamma B_2}{2} - \mu & \alpha - 1 & \frac{\gamma(B_3 - B_1)}{2} & \frac{\gamma(A_3 - A_1)}{2} & \dots & 0 \\ \gamma A_2 & \frac{\gamma(A_3 + A_1)}{2} & \frac{\gamma(B_3 - B_1)}{2} & \alpha - 4 & 2\mu + \frac{\gamma B_2}{2} & \dots & 0 \\ \dots & \dots & \dots & \dots & \dots & \dots & \dots \end{bmatrix} \begin{bmatrix} \alpha_0 \\ \alpha_1 \\ \alpha_2 \\ b_2 \\ a_3 \\ \dots \end{bmatrix} = 0$$

$$\begin{bmatrix} \alpha + \alpha - \frac{1}{4} + \frac{\gamma A_1}{2} & \frac{\gamma B_1}{2} + \frac{\mu}{2} & \frac{\gamma(A_2 + A_1)}{2} & \frac{\gamma(B_2 + B_1)}{2} & \frac{\gamma(A_2 + A_3)}{2} & \dots & 0 \\ \gamma B_1 - \frac{\mu}{2} & \alpha - \frac{1}{4} - \frac{\gamma A_1}{2} & \frac{\gamma(B_2 - B_1)}{2} & \frac{\gamma(A_2 - A_1)}{2} & \frac{\gamma(B_3 - B_2)}{2} & \dots & 0 \\ \frac{\gamma(A_2 + A_1)}{2} & \frac{\gamma(B_2 - B_1)}{2} & \alpha - \frac{9}{4} + \frac{\gamma A_3}{2} & \frac{\gamma(B_3)}{2} + \frac{3\mu}{2} & \frac{\gamma(A_4 + A_1)}{2} & \dots & 0 \\ \frac{\gamma(B_2 + B_1)}{2} & \frac{\gamma(A_2 - A_1)}{2} & \frac{\gamma(B_3)}{2} - \frac{3\mu}{2} & \alpha - \frac{9}{4} - \frac{\gamma A_3}{2} & \frac{\gamma(B_2 - B_1)}{2} & \dots & 0 \\ 0 & 0 & \dots & \dots & \dots & \dots & \dots \end{bmatrix} \begin{bmatrix} \alpha_0 \\ \alpha_1 \\ \alpha_2 \\ b_2 \\ a_3 \\ \dots \end{bmatrix} = 0 \tag{B.3}$$

Neglecting the trivial solution we see that the Hill’s determinant should be equal to zero for the equations to hold. Thus we obtain the relationship between the parameters α , γ and the damping coefficient which can be plotted in the parameter space to obtain the curves of marginal stability for the damped Hill’s equation. Comparing the parametric matrices of Hill’s equation (Eqs. (B.2) and (B.3)) to that of Mathieu’s equation (Eqs. (A.4) and (A.5)) we see that the coefficients of higher harmonics in the Hill’s equation populate the parametric matrices of the Mathieu’s equation. In this manner we incorporate the actual variation in the stiffness into the Hill’s determinant. Thus the Ince-Strutt diagram developed for Hill’s equation will be specific to the system and will change according to the system stiffness.

Now we have a much more accurate model which is system specific and the marginal stability boundaries are more realistic and accurate. It is also interesting to note that we can obtain the

corresponding Hill's determinant for Mathieu's equation from that for Hill's equation by setting the higher harmonic coefficients ($B_1, A_2, B_2...$) equal to zero. This confirms the consistency of the method.